*Journal of Ceramic Processing Research. Vol. 14, Special. 1, pp. s26~s29 (2013)*

J O U R N A L O F
**Ceramic Processing Research**

# Synthesis of carboxylate-intercalated layered yttrium hydroxides by anion exchange reactions and their application to $Ln^{3+}$-activated luminescent materials

**Kaori Sakuma and Shinobu Fujihara***

*Department of Applied Chemistry, Faculty of Science and Technology, Keio University, 3-14-1 Hiyoshi, Kohoku-ku, Yokohama 223-8522, Japan*

**Layered yttrium hydroxide compounds based on $Eu^{3+}$-and/or $Tb^{3+}$-doped $Y_2(OH)_5NO_3 \cdot nH_2O$ were synthesized in aqueous solutions containing hexamethylenetetramine. Nitrate ions were then exchanged with carboxylate ions such as 4-biphenylacetate (BPA), benzoate, terephthalate, maleate, or oxalate, which were successfully intercalated between yttrium hydroxide layers. While the initial $Eu^{3+}$- or $Tb^{3+}$-doped nitrate samples suffered from relatively low photoluminescence (PL) intensity, those intercalated with BPA, benzoate, terephthalate, or oxalate ions showed considerably enhanced PL intensity, accompanying with broad excitation bands at around 220 - 300 nm. This enhancement was explained with the so-called antenna effect of the organic species. In the $Eu^{3+}$-$Tb^{3+}$-codoped samples, the antenna effect worked similarly for $Eu^{3+}$ and $Tb^{3+}$, thereby resulting in their simultaneous emissions at a single excitation wavelength.**

**Key words: Layered compounds, Intercalation, Antenna effect, Photoluminescence.**

## Introduction

Layered rare-earth hydroxides (LRHs), expressed with a general formula of $Ln_2(OH)_5X \cdot nH_2O$ ($Ln^{3+}$ = rare-earth cations and $X^-$ = intercalated anions), have been recognized as a series of newly emerged inorganic layered compounds [1-3]. Although the LRHs are structurally analogous to the well-known layered double hydroxides (LDHs), $M^{2+}_{1-x}M^{3+}_x(OH)_2(A^{n-})_{x/n}mH_2O$ ($A^{n-}$ = intercalated anions), the LRHs basically have only one type of cations in the metal hydroxide layer. Due to the presence of rare-earth cations, the LRHs exhibit unique electronic, magnetic, catalytic, and optical properties coming from incompletely filled 4f-orbitals [4]. One of the advantages of using the LRHs as functional materials is that they are compositionally flexible in terms of their layer compositions. As a result, both chemical and physical properties can possibly be tuned by the kind of inorganic and organic anions that are intercalated between layers. We have focused on $Y_2(OH)_5NO_3 \cdot nH_2O$, which is one of the representative LRHs, because it can be applied to luminescent materials by replacing $Y^{3+}$ with $Ln^{3+}$ activators [5]. Moreover, anion exchange reactions of $NO_3^-$ with various organic anions have been successfully carried out to modulate its physical and chemical properties [1, 3, 6]. In this study, we synthesized layered yttrium hydroxides (LYHs) where 4-biphenylacetate ($C_6H_5C_6H_4CH_2COO^-$), benzoate ($C_6H_5COO^-$), terephthalate ($C_6H_4(COO)_2^{2-}$), maleate ($C_2H_2(COO)_2^{2-}$), or oxalate ($(COO)_2^{2-}$) ions were intercalated between layers by anion exchange reactions of $Y_2(OH)_5NO_3 \cdot nH_2O$. Influences of the interlayer anions on luminescent properties of $Eu^{3+}$-doped, $Tb^{3+}$-doped, or $Eu^{3+}$-$Tb^{3+}$-codoped LYHs were then systematically investigated.

*Corresponding author:
Tel : +81-45-566-1581
Fax: +81-45-566-1551
E-mail: shinobu@applc.keio.ac.jp

## Experimental

20 ml of aqueous $Eu(NO_3)_3 \cdot 6H_2O$ and/or $Tb(NO_3)_3 \cdot 6H_2O$ solutions with $Ln^{3+}$ dopant concentrations of 2, 4, 5, 6, or 8 mol% against yttrium or 20 ml of deionized water (for preparing samples without rare-earth doping) was mixed with 40 ml of an aqueous $Y(NO_3)_3 \cdot nH_2O$ solution (0.15 M). 24 mmol of hexamethylenetetramine was added to the solutions, followed by stirring for 30 min at room temperature. Powdery products were precipitated during keeping the solutions at 90 °C for 3 h. Undoped and doped LYH samples were obtained through filtering, washing, and drying at 60 °C. For the anion exchange reaction, 0.2 g of the LYH sample was dispersed in 10 or 30 ml of aqueous solutions containing 6 mmol of sodium benzoate, disodium terephthalate, disodium maleate, or disodium oxalate. In case of 4-biphenylacetic acid (BPA), 0.95 mmol of BPA was dissolved in 10 ml of NaOH (0.1 M). The resultant suspensions were stirred for 24 h at room temperature. For the maleate sample, the suspension was kept at 60 °C for 168 h. The suspensions were then filtered, washed, and dried at 60 °C. The samples are designated in order of the kind of the dopants, the concentration in mol%, and the intercalated anions. E, T, ET, and N stand for $Eu^{3+}$-doping, $Tb^{3+}$-doping, $Eu^{3+}$-$Tb^{3+}$-codoping,

and no-doping, respectively. For instance, "E5-(benzoate)" represents the sample doped with 5 mol% of $Eu^{3+}$ and intercalated with the benzoate ion.

The phase identification and structural analysis of the LYH samples were performed with an X-ray diffractometer using CuKα radiation (Bruker AXS, type D8 Advance). Photoluminescence (PL) spectra were measured at room temperature with a spectrofluorophotometer (JASCO, type FP-6500) using a xenon lamp (150 W) as a light source. The organic species present in the samples were examined by Fourier transform infrared (FT-IR) spectroscopy (Varian, type FTS-60A/896) using a KBr method. The thermal decomposition behavior of the samples was examined by thermogravimetry-differential thermal analysis (TG-DTA) with a Mac Science 2020S analyzer. Diffuse reflectance spectra were recorded with an ultraviolet (UV)-visible spectrophotometer (JASCO, type V-670) using an integrating sphere unit (JASCO, type ISN-723).

## Results and Discussion

Fig. 1 shows X-ray diffraction (XRD) patterns of the non-doped LYH samples with N-(nitrate), N-(BPA), N-(benzoate), N-(terephthalate), N-(maleate), and N-(oxalate). The pattern of the N-(nitrate) is indexed with a $Y_2(OH)_{5.14}(NO_3)_{0.86}\cdot H_2O$ phase (ICDD 32-1435). The presence of the nitrate ion was also confirmed by FT-IR for the N-(nitrate). Patterns of the doped LYH samples with E-(nitrate), T-(nitrate), and ET-(nitrate) were similar to that of the N-(nitrate). According to the TG-DTA analysis of the N-(nitrate), endothermic peaks were observed at 77, 275, and 492 °C, accompanied by three steps of weight losses, which were attributed to the following chemical reactions [1]:

$$Y_2(OH)_5NO_3\cdot nH_2O \rightarrow Y_2(OH)_5NO_3 + nH_2O \quad (1)$$
$$Y_2(OH)_5NO_3 \rightarrow Y_2O_2(OH)NO_3 + 2H_2O \quad (2)$$
$$Y_2O_2(OH)NO_3 \rightarrow Y_2O_3 + 0.5H_2O + NO_2 + 0.25O_2 \quad (3)$$

The number of the hydrate water (n) was determined to be 1.84 in our $Y_2(OH)_5NO_3\cdot nH_2O$ sample from the first weight loss. Thus the N-(nitrate) sample is actually characterized as layered yttrium hydroxide nitrate containing the hydrate water.

A half of the interlayer distance in the N-(nitrate) is 0.930 nm, as determined from the (002) peak of the XRD pattern. In the anion-exchanged samples, the (002) peak is shifted and a half of the interlayer distance is determined to be 2.439, 1.719, 1.271, 1.081, and 0.795 nm for N-(BPA), N-(benzoate), N-(terephthalate), N-(maleate), and N-(oxalate), respectively, as shown in Fig. 1. The apparently decreased half of the interlayer distance of N-(oxalate) corresponds to the actual interlayer distance of $Y_2(OH)_5(C_2O_4)_{0.5}\cdot H_2O$ reported in the literature [1]. In the FT-IR analysis, we confirmed the appearance of symmetric and asymmetric $COO^-$ stretching vibrations from the respective organic anions. In the TG-DTA analysis of N-(BPA), N-(benzoate), and N-(terephthalate), exothermic peaks appeared at 400 - 500, 400 - 460, and 400 - 550 °C, respectively, which was attributed to the combustion of the respective intercalated anions. In the case of N-(maleate) and N-(oxalate), no clear exothermic peaks were observed. However, for the samples obtained by heating N-(maleate) and N-(oxalate) at 400 °C for 1 h, the presence of the $COO^-$ was still observed in the FT-IR analysis.

PL excitation and emission spectra of E5-(nitrate) and E5-(benzoate) are shown in Fig. 2. In the emission spectra, $^5D_0 \rightarrow {}^7F_J$ (J = 0, 1, 2, 3, and 4) transitions of $Eu^{3+}$ are observed at 579, 589 - 595, 615, 650, and 698 nm, respectively, and the electric-dipole $^5D_0 \rightarrow {}^7F_2$ transition gives the highest intensity for both the samples. The excitation spectrum of E5-(nitrate) for the 615 nm emission has only a predominant peak at 395 nm, which corresponds to the direct $^7F_0 \rightarrow {}^5L_6$ excitation of $Eu^{3+}$. In contrast, E5-(benzoate) exhibits an intense and broad excitation band ranging from 220 to 300 nm. The excitation at a peak wavelength (280 nm) then results in the much higher PL emission

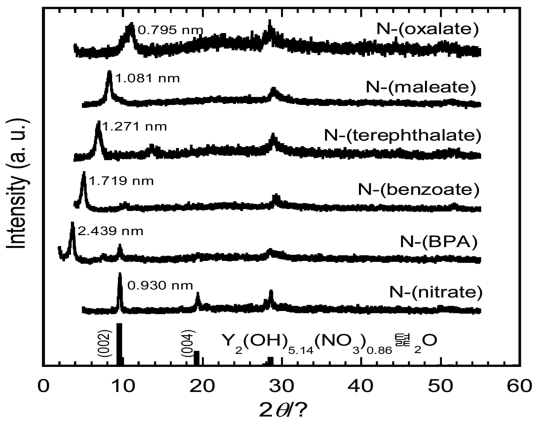


**Fig. 1.** XRD patterns of the non-doped LYH samples of N-(nitrate), N-(BPA), N-(benzoate), N-(terephthalate), N-(maleate), and N-(oxalate).

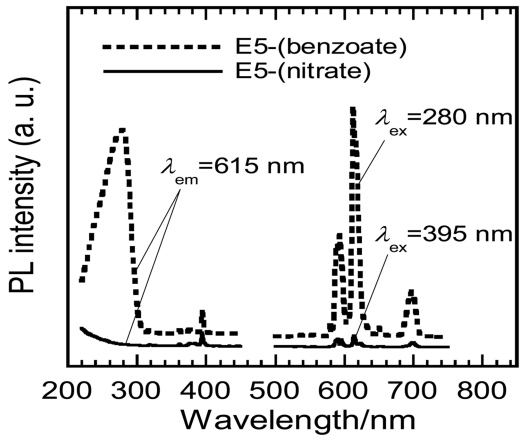


**Fig. 2.** PL excitation and emission spectra of the $Eu^{3+}$(5 mol%)-doped LYH samples of E5-(nitrate) and E5-(benzoate).

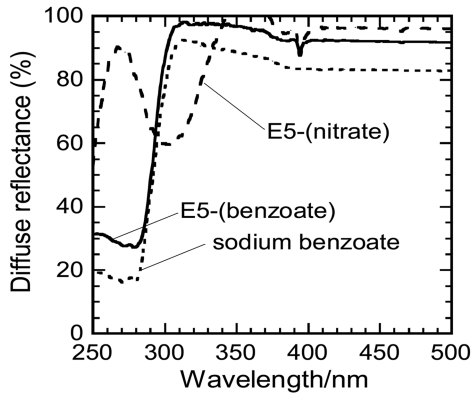


**Fig. 3.** Diffuse reflectance spectra of the $Eu^{3+}$(5 mol%)-doped LYH samples of E5-(nitrate) and E5-(benzoate), together with sodium benzoate.

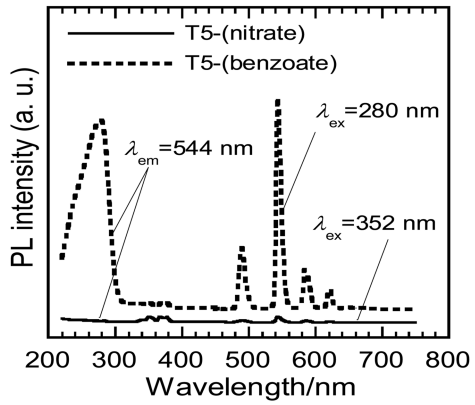


**Fig. 4.** PL excitation and emission spectra of the $Tb^{3+}$(5 mol%)-doped LYH samples of T5-(nitrate) and T5-(benzoate).

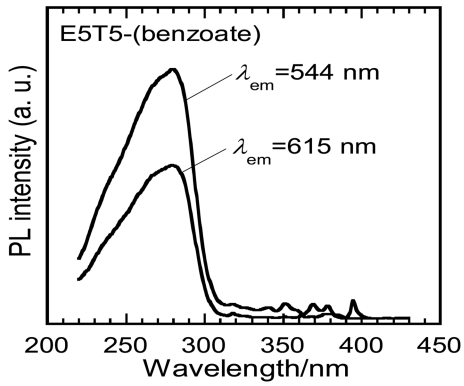


**Fig. 5.** PL excitation spectra of the $Eu^{3+}$(5 mol%)- and $Tb^{3+}$(5 mol%)-codoped LYH sample of E5T5-(benzoate).

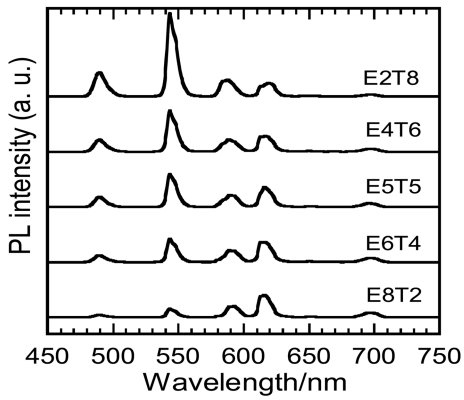


**Fig. 6.** PL emission spectra of the $Eu^{3+}$- and $Tb^{3+}$-codoped LYH samples of E2T8-, E4T6-, E5T5-, E6T4-, and E8T2-(benzoate).

intensity in E5-(benzoate). To examine the light absorption, diffuse reflectance spectra of E5-(nitrate), E5-(benzoate), and sodium benzoate were measured and results are compared in Fig. 3. E5-(benzoate), as well as sodium benzoate, shows intense absorption in the UV region below 305 nm, which is attributed to the transition of the benzene ring [7, 8]. It is then considered that the excitation is achieved with an efficient energy transfer from the intercalated benzoate ions to the $Eu^{3+}$ ions located in the yttrium hydroxide layers. This excitation mechanism is apparently similar to the antenna effect which is observed in the organic ligand acting as a photon collector (chromophore) [9]. Actually, the organic ligand absorbs light due to a singlet singlet transition. The excited singlet state of the ligand relaxes non-radiatively to its triplet state and its energy is transferred to the $Ln^{3+}$ ions. The antenna effect has been observed in $Ln_2(TerePhth)_3(H_2O)_4$ (TerePhth = terephthalate) [9], amorphous zinc benzoate doped with $Ln^{3+}$ [8], and benzoic acid-modified $CaF_2$:$Ln^{3+}$ nanoparticles [10].

Fig. 4 shows PL excitation and emission spectra of T5-(nitrate) and T5-(benzoate). Emissions due to $^5D_4 \rightarrow {}^7F_J$ (J = 6, 5, 4, and 3) transitions of $Tb^{3+}$ are observed at 490, 544, 586, 621 nm, respectively. Similarly to the case of europium, T5-(nitrate) has much lower PL intensity than T5-(benzoate). Furthermore, T5-(benzoate) exhibits almost the same excitation spectrum for the 544 nm emission as that of E5-(benzoate). Since we confirmed the absorption due to the benzoate ions in diffuse reflectance of T5-(benzoate), it is said that the antenna effect works also for the doped $Tb^{3+}$ ions. The other LYH samples showed as well broad excitation bands at 220 - 350 nm for E-(BPA) and T-(BPA), 220 -330 nm for E-(terephthalate) and T-(terephthalate), and 220 - 310 nm for E-(oxalate) and T-(oxalate) with various doping concentrations, accompanied by intense PL emissions. In case of E-(maleate) and T-(maleate), however, it appeared that the effective excitation was not allowed through the antenna effect. As mentioned in the experimental part, the exchange of the maleate was relatively difficult and the suspension had to be kept at 60 ºC for 168 h. We assume that the chemical bonding between the maleate ions and the hydroxide layers is not built well in E-(maleate) and T-(maleate).

It is an interesting undertaking to dope $Eu^{3+}$ and $Tb^{3+}$ simultaneously in the carboxylate-intercalated LYHs because they might be excited at a single wavelength. Fig. 5 shows PL excitation spectra of E5T5-(benzoate) for the 544 ($Tb^{3+}$) and the 615 nm ($Eu^{3+}$) emission.

Broad excitation bands are observed at the same wavelengths in the UV region for both the emissions. The PL excitation intensity of $Tb^{3+}$ is higher than that of $Eu^{3+}$ at the same doping level. Similar results were obtained for the other samples of E5T5-(BPA), E5T5-(terephthalate), and E5T5-(oxalate). Fig. 6 shows PL emission spectra of a series of $Eu^{3+}$-$Tb^{3+}$-codoped LYH samples (E2T8-, E4T6-, E5T5-, E6T4-, and E8T2-(benzoate)). The $Eu^{3+}$ emission peaks are located at 615, 650, and 698 nm and the $Tb^{3+}$ emission peaks at 490, 544, and 586 nm. While a change of the PL intensity of the $Eu^{3+}$ emissions is relatively small among the samples, that of the $Tb^{3+}$ emissions is relatively large with decreasing its concentration from 8 to 2 mol%. The same trend was also observed in a series of the terephthalate-intercalated samples. This may indicate that the antenna effect is more remarkable with the $Tb^{3+}$ ions. The emission color of samples intercalated with the benzoate or terephthalate ions could be finely tuned from green to yellow and red by varying the $Tb^{3+}$ and $Eu^{3+}$ concentrations. Our results demonstrate that the intercalation of the carboxylate ions and the codoping of $Tb^{3+}$ and $Eu^{3+}$ are the attractive way to modulate luminescent properties of the layered yttrium hydroxide materials.

## Conclusions

We synthesized $Eu^{3+}$- and/or $Tb^{3+}$-doped $Y_2(OH)_5NO_3 \cdot 1.84H_2O$ where BPA, benzoate, terephthalate, maleate, or oxalate anions were intercalated between the yttrium hydroxide layers by anion exchange reactions. The samples intercalated with BPA, benzoate, terephthalate, or oxalate ions showed the broad excitation bands in the PL excitation spectra, followed by the enhanced PL emissions. The enhancement was explained with the antenna effect due to the UV light absorption by organic species and the subsequent energy transfer to the doped $Eu^{3+}$ or $Tb^{3+}$ ions. The simultaneous emissions from $Eu^{3+}$ and $Tb^{3+}$ were observed at the single excitation wavelength in the codoped samples.

## References

1. L.J. McIntyre, L.K. Jackson, and A.M. Fogg, J. Phys. Chem. Solids 69 (2008) 1070-1074.
2. S.A. Hindocha, L.J. McIntyre, and A.M. Fogg, J. Solid State Chem. 182 (2009) 1070-1074.
3. Y. Xi, and R.J. Davis, Inorg. Chem. 49 (2010) 3888-3895.
4. Q. Zhu, J.G. Li, C. Zhi, R. Ma, T. Sasaki, J.X. Xu, C.H. Liu, X.D. Li, X.D. Sun, and Y. Sakka, J. Mater. Chem. 21 (2011) 6903-6908.
5. Q. Zhu, J.G. Li, C. Zhi, X. Li, X. Sun, Y. Sakka, D. Golberg, and Y. Bando, Chem. Mater. 22 (2010) 4204-4213.
6. K.H. Lee, and S.H. Byeon, Eur. J. Inorg. Chem. (2009) 929-936.
7. M. Ito, J. Mol. Spectr. 4 (1960) 144-154.
8. L. Yuan, J. Sun, and K. Zhang, Spectrochim. Acta. A 59 (2003) 729-731.
9. M. Hilder, P.C. Junk, U.H. Kynast, and M.M. Lezhnina, J. Photochem. Photobiol. A-Chem. 202 (2009) 10-20.
10. J. Wang, Z. Wang, X. Li, S. Wang, H. Mao, and Z. Li, Appl. Surf. Sci. 257 (2011) 7145-7149.